

## Experimental and Theoretical Characterization of $\text{H}_2\text{OOO}^+$

Mingfei Zhou,<sup>\*,†</sup> Aihua Zeng,<sup>†</sup> Yun Wang,<sup>†</sup> Qingyu Kong,<sup>†</sup> Zhi-Xiang Wang,<sup>‡</sup> and Paul van Rague Schleyer<sup>‡</sup>

Shanghai Key Laboratory of Molecular Catalysts and Innovative Materials, Department of Chemistry & Laser Chemistry Institute, Fudan University, Shanghai 200433, P.R. China, and Center for Computational Quantum Chemistry, Computational Chemistry Annex, University of Georgia, Athens, Georgia 30602-2525

Received July 8, 2003; E-mail: mzfzhou@fudan.edu.cn

Detailed knowledge concerning the interaction between water and oxygen is of fundamental importance in biological, atmospheric, and environmental sciences. For instance, photonucleation, an important atmospheric phenomenon, was proposed to involve the initial formation of a van der Waals complex,  $[\text{H}_2\text{O}\cdot\text{O}_2]$ , followed by its conversion into a charge-transfer complex,  $[\text{H}_2\text{O}^+\text{O}_2^-]$ , upon UV irradiation.<sup>1,2</sup> Antibodies use  $\text{H}_2\text{O}$  as an electron source in biological systems. This facilitates the interaction of water with singlet  $\text{O}_2$  to form  $\text{H}_2\text{O}_3$ , the first intermediate in a reaction cascade which eventually gives  $\text{H}_2\text{O}_2$ .<sup>3,4</sup> The  $[\text{H}_2\text{O}\cdot\text{O}_2]^+$  ion, existing in the ionosphere, is assumed to be an important intermediate in the formation of proton hydrates,  $\text{H}^+(\text{H}_2\text{O})_n$ ,<sup>5–10</sup> from  $\text{O}_2^+$ . The kinetics and mechanism of photodissociation of the  $[\text{H}_2\text{O}\cdot\text{O}_2]^+$  cation have been studied, and, without sophisticated characterization, the cation was assumed to be an ion–molecule complex depicted as  $\text{O}_2^+\cdot\text{H}_2\text{O}$ .<sup>5–10</sup> We now characterize the  $[\text{H}_2\text{OOO}]^+$  cation spectroscopically as well as theoretically and show that a 3c–1e bond is involved, instead of a simple ion–molecule complex.

The  $\text{H}_2\text{OOO}^+$  cation was prepared by condensation of  $\text{H}_2\text{O}/\text{Ar}$  and  $\text{O}_2/\text{Ar}$  via radio frequency discharge. Briefly, two separated gas streams containing  $\text{O}_2/\text{Ar}$  and  $\text{H}_2\text{O}/\text{Ar}$  were co-deposited onto a 4 K CsI window simultaneously. One of the gas streams was subjected to discharge from a Tesla coil. The  $\text{H}_2\text{O}/\text{Ar}$  (1:500 to 1:100) and  $\text{O}_2/\text{Ar}$  (1:50 to 1:100) mixtures were prepared from distilled water and high purity oxygen and argon. Infrared spectra were recorded on a Bruker Equinox 55 spectrometer at 0.5  $\text{cm}^{-1}$  resolution using a DTGS detector.

Condensation of the  $\text{H}_2\text{O}/\text{Ar}$  products at 4 K after discharge resulted in OH (3547.9  $\text{cm}^{-1}$ ),<sup>11</sup> HOO (3412.1, 1388.3, and 1100.7  $\text{cm}^{-1}$ ),<sup>12,13</sup>  $\text{H}_2\text{O}\cdot\text{OH}$  (3451.6  $\text{cm}^{-1}$ ),<sup>14</sup> and unidentified 767.8  $\text{cm}^{-1}$  absorptions. Similarly,  $\text{O}_3$  (1039.4  $\text{cm}^{-1}$ ),  $\text{O}_3^-$  (803.9  $\text{cm}^{-1}$ ),<sup>15</sup>  $\text{O}_4^-$  (953.6  $\text{cm}^{-1}$ ),<sup>16</sup> and  $\text{O}_4^+$  (1118.4  $\text{cm}^{-1}$ )<sup>17</sup> were produced after discharge of  $\text{O}_2/\text{Ar}$  and condensation. New absorptions were observed when  $\text{H}_2\text{O}/\text{Ar}$  was co-deposited with discharged  $\text{O}_2/\text{Ar}$ . The same new absorptions were produced when  $\text{H}_2\text{O}/\text{Ar}$  was subjected to discharge and co-deposited with  $\text{O}_2/\text{Ar}$ . These bands can be grouped together by their consistent behavior upon annealing and photolysis. The spectra in the O–H stretching frequency region are shown in Figure 1. The new product absorptions diminished after the sample was annealed to 20 K or after broadband Hg arc lamp photolysis (Figure 1, spectrum b). When  $\text{CCl}_4$  was added to serve as an electron trap,<sup>18</sup> the intensities of the new product absorptions were increased relative to the neutral  $\text{H}_2\text{O}\cdot\text{OH}$  and HOO absorptions (Figure 1, spectrum c), while the  $\text{O}_3^-$  and  $\text{O}_4^-$  anions were eliminated. These results suggest that the new product is a cationic species.

Isotopic substitutions ( $\text{D}_2\text{O}$ ,  $\text{H}_2^{18}\text{O}$ ,  $^{18}\text{O}_2$ , and their mixtures) were employed for product identification based on isotopic shifts and

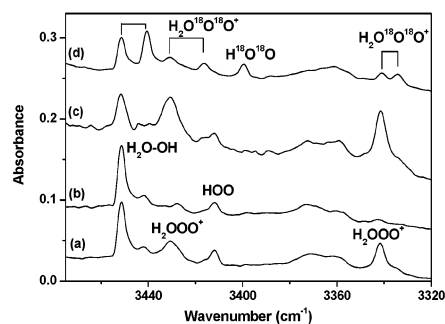


**Figure 1.** IR spectra in the 3475–3320  $\text{cm}^{-1}$  region from co-deposition of  $\text{H}_2\text{O}/\text{Ar}$  with discharged  $\text{O}_2/\text{Ar}$  at 4 K. (a) 1.0%  $\text{H}_2\text{O}/\text{Ar}$  and 1.5%  $\text{O}_2/\text{Ar}$ , deposited sample, (b) spectrum after irradiation at  $\lambda > 250$  nm, (c) 1.0%  $\text{H}_2\text{O} + 0.1\%$   $\text{CCl}_4/\text{Ar}$  and 1.5%  $\text{O}_2/\text{Ar}$ , deposited sample, and (d) 0.5%  $\text{H}_2^{16}\text{O} + 0.5\%$   $\text{H}_2^{18}\text{O}/\text{Ar}$  and 1.5%  $^{18}\text{O}_2/\text{Ar}$ , deposited sample.

**Table 1.** Infrared Absorptions (in  $\text{cm}^{-1}$ ) Observed for Various  $\text{H}_2\text{OOO}^+$  Isotopomers in Solid Argon

	OH asy str.	OH sym. str.	O–O str.	$\text{H}_2\text{O}-\text{O}_2$ str.
$\text{H}_2\text{OOO}^+$	3430.7	3341.7		731.0
$\text{D}_2\text{OOO}^+$	2555.5	2449.6	1601.1	606.3
$\text{H}_2\text{O}^{18}\text{O}^{18}\text{O}^+$	3430.4	3341.0	1502.2	726.8
$\text{H}_2^{18}\text{OOO}^+$	3416.2	3334.9		724.2
$\text{D}_2\text{O}^{18}\text{O}^{18}\text{O}^+$	2555.4	2449.0	1511.4	598.7
HDOOO <sup>+</sup>	3383.8	2499.7		
HDO <sup>18</sup> O <sup>18</sup> O <sup>+</sup>	3384.0	2499.7	1515.9	

absorption splitting. The infrared absorptions with different isotopic samples are listed in Table 1. The 3341.7 and 3430.7  $\text{cm}^{-1}$  bands exhibit  $\text{H}_2\text{O}/\text{D}_2\text{O}$  (1.3642 and 1.3425) and  $\text{H}_2^{16}\text{O}/\text{H}_2^{18}\text{O}$  frequency ratios (1.0020 and 1.0042) that are characteristic of symmetric and antisymmetric HOH stretching vibrations. The mixed  $\text{H}_2^{16}\text{O} + \text{H}_2^{18}\text{O}$  (Figure 1, spectrum d) and  $\text{H}_2\text{O} + \text{HDO} + \text{D}_2\text{O}$  (Figure 1 of Supporting Information) spectra clearly show that one  $\text{H}_2\text{O}$  unit with two equivalent H atoms is involved in these two modes. The strong  $\text{H}_2\text{O}$  bending vibration overlaps the O–O stretching mode of  $\text{H}_2\text{OOO}^+$ . Yet the corresponding modes of the  $\text{D}_2\text{OOO}^+$  and  $\text{H}_2\text{O}^{18}\text{O}^{18}\text{O}^+$  isotopomers are observed distinctly at 1601.1 and 1502.2  $\text{cm}^{-1}$  (Figure 2 of Supporting Information). This mode shows small isotopic shifts with  $\text{D}_2\text{O}$  and  $\text{H}_2^{18}\text{O}$ . The mixed  $^{16}\text{O}_2 + ^{18}\text{O}_2$  and  $^{16}\text{O}_2 + ^{16}\text{O}^{18}\text{O} + ^{18}\text{O}_2$  spectra indicate that one  $\text{O}_2$  unit with slightly nonequivalent O atoms is involved in this mode. That the O–O stretching frequencies of  $\text{H}_2\text{O}^{18}\text{O}^{18}\text{O}^+$  are lower than those of  $\text{D}_2\text{O}^{18}\text{O}^{18}\text{O}^+$  and  $\text{HDO}^{18}\text{O}^{18}\text{O}^+$  suggests that this mode for the last two isotopomers is involved in anharmonic resonance with a combination of lower-lying levels. The less prominent 731.0  $\text{cm}^{-1}$  band is assigned to the  $\text{H}_2\text{O}-\text{O}_2$  stretching vibration of the cation.

After this  $\text{H}_2\text{OOO}^+$  radical cation was fingerprinted spectroscopically, quantum chemical computations gave insight into the

<sup>†</sup> Fudan University.  
<sup>‡</sup> University of Georgia.

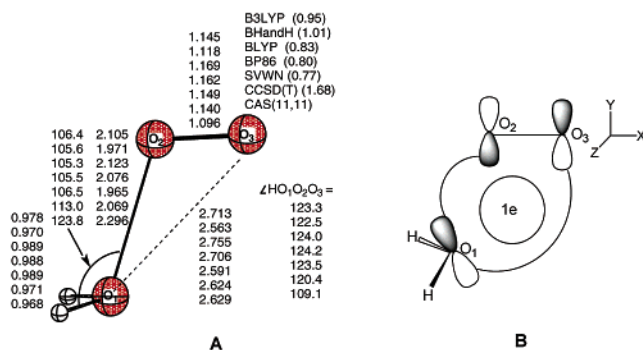


**Figure 2.** (A) Geometries calculated at various levels (bond length in Å, bond angle in deg). (B) Interaction between the  $\pi_y^*$  of  $\text{O}_2^+$  and in-plane water lone pair. The values in parentheses are  $S^2$  values.

**Table 2.** Comparison of Calculated and Observed IR Frequencies (in  $\text{cm}^{-1}$ ) for  $\text{H}_2\text{OOO}^+$  (Values in Parentheses Are IR Intensities)

	OH asy str.	OH sym. str.	O–O str.	$\text{H}_2\text{O}-\text{O}_2$ str.
B3LYP	3723(238)	3621(535)	1762(593)	679(133)
BHHLYP	3861(320)	3746(884)	1860(1423)	687(109)
BLYP	3587(206)	3490(340)	1645(240)	689(167)
BP86	3615(211)	3516(323)	1694(219)	711(169)
SVWN	3624(271)	3521(349)	1773(186)	745(190)
CCSD(T)	3836	3738	1820	647
observed	3430.7	3341.7	1601.1 <sup>a</sup>	731.0

<sup>a</sup> The  $\text{D}_2\text{OOO}$  value. The frequency for  $\text{H}_2\text{OOO}$  is expected to be 2–3  $\text{cm}^{-1}$  higher.

nature of the bonding.<sup>19</sup> The optimized geometries at various levels of theory are given in Figure 2A, and the computed harmonic frequencies are compared with the experimental values in Table 2. At all levels employed, the radical has a doublet ground state ( $^2A''$ ) structure with  $C_3$  symmetry which correlates with  $\text{H}_2\text{O} + \text{O}_2^+$ . As shown in Figure 2B, the empty  $\pi_y^*$  orbital of  $\text{O}_2^+$  (the singly occupied  $\pi_y^*$  in the ground state of  $\text{O}_2^+$ ) interacts with an in-plane water lone pair orbital favorably. The single electron occupying this orbital glues  $\text{O}_2^+$  and  $\text{H}_2\text{O}$  together. The Wiberg bond indices of  $\text{O}_1\text{O}_2$  and  $\text{O}_1\text{O}_3$  are 0.26 and 0.21, and the  $\text{O}_2$  and  $\text{H}_2\text{O}$  fragment charges are +0.59 and +0.41e, respectively. Therefore, this radical is a complex involving a  $3c-1e$  bond, rather than a simple ion–molecule complex,  $\text{O}_2^+\text{H}_2\text{O}$ . The calculated isotopic frequency ratios (Table 2 of Supporting Information) are in good agreement with the experimental values, which add strong support to the experimental assignment.

The  $\text{O}_1-\text{O}_2$  stretching vibrational frequency is an important characteristic of the interaction between the two fragments. Mainly due to the neglect of anharmonicity, computed vibrational frequencies are generally higher than the experimental values. While the OH symmetric stretching, OH antisymmetric stretching, and  $\text{O}_2-\text{O}_3$  stretching frequencies follow this generalization (Table 2), the  $\text{O}_1-\text{O}_2$  stretching frequency is underestimated. Thus, the computed hybrid B3LYP (679  $\text{cm}^{-1}$ ) and BHHLYP (687  $\text{cm}^{-1}$ ) values are smaller than the experimental value of 731  $\text{cm}^{-1}$ . The gradient-corrected BLYP and BP86 values of 689 and 711  $\text{cm}^{-1}$ , respectively, are closer. The CCSD(T) “panacea” did not improve the agreement. We attribute this to the large spin contamination: the  $S^2 = 1.68$  value for the doublet is quite large. Surprisingly, the simpler SVWN/6-311++G\*\* method, which generally is less accurate than hybrid and gradient-corrected DFT, performs well and gives a 745  $\text{cm}^{-1}$  frequency. As has been discussed in several papers,<sup>20,21</sup> DFT methods suffer from self-interaction errors in describing radical cations with odd electron bonds (e.g., hemibonds). However, the simpler LSD method is known to perform better for hemi-bonded species.<sup>21</sup> Therefore, the  $\text{O}_1\text{O}_2$  bond length (1.965 Å)

predicted by SVWN/6-311++G\*\* may be more accurate than the CCSD(T) and the other DFT distances, which may overestimated. The overly long (2.296 Å) separation predicted by CASSCF(11,11)/6-311G\*\* evidently is due to the lack of dynamic electron correlation. These problems – self-interaction error in DFT, large spin contamination in CCSD(T), and lack of dynamic correlation in CASSCF – might, in principle, be overcome at multireference levels, such as MRSDCI and MRCI-SD/AQCC, but optimization and frequency computations are not feasible at present.

In summary, we have characterized  $\text{H}_2\text{OOO}^+$  to be a complex involving a  $3c-1e$  bond, instead of a simple ion–molecule complex. The  $\text{H}_2\text{OOO}^+$  cation is stable under visible irradiation; it only was destroyed by UV photolysis. However, the cation absorption diminished quickly on annealing, suggesting high reactivity toward, for example,  $\text{O}_2$  or  $\text{H}_2\text{O}$ .

**Acknowledgment.** The NSFC (20125033), the NKBRSF, and the University of Georgia supported this work. We thank Hans Lischka for attempting multireference calculations, and H. F. Schaefer, III and the referees for helpful discussions.

**Supporting Information Available:** Spectra and calculated vibrational frequencies and intensities (PDF). This material is available free of charge via the Internet at <http://pubs.acs.org>.

## References

- Byers Brown, W. *Chem. Phys. Lett.* **1995**, *235*, 94.
- Cacace, F.; de Petris, G.; Pepi, F.; Troiani, A. *Angew. Chem., Int. Ed.* **2000**, *39*, 367.
- Wentworth, P., Jr.; Jones, L. H.; Wentworth, A. D.; Zhu, X.; Larsen, N. A.; Wilson, I. A.; Xu, X.; Goddard, W. A.; Janda, K. D.; Eschenmoser, A.; Lerner, R. A. *Science* **2001**, *293*, 1806.
- Engdahl, A.; Nelander, B. *Science* **2002**, *295*, 482.
- Fehsenfeld, F. C.; Mosesman, M.; Ferguson, E. E. *J. Chem. Phys.* **1971**, *55*, 2115.
- Howard, C. J.; Bierbaum, V. M.; Rundle, H. W.; Kaufman, F. *J. Chem. Phys.* **1972**, *57*, 3491.
- Smith, G. P.; Lee, L. C. *J. Chem. Phys.* **1978**, *69*, 5393.
- Beyer, R. A.; Vanderhoff, J. A. *J. Chem. Phys.* **1976**, *65*, 2313.
- McCrum, J. L. *Planet. Space Sci.* **1982**, *30*, 559.
- Angel, L.; Stace, A. J. *J. Phys. Chem. A* **1999**, *103*, 2999.
- Cheng, B. M.; Lee, Y. P.; Ögilvie, J. F. *Chem. Phys. Lett.* **1988**, *151*, 109.
- Milligan, D. E.; Jacox, M. E. *J. Chem. Phys.* **1963**, *38*, 2627.
- Smith, D. W.; Andrews, L. *J. Chem. Phys.* **1974**, *60*, 81.
- (a) Langford, V. S.; McKinley, A. J.; Quickenden, T. I. *J. Am. Chem. Soc.* **2000**, *122*, 12859. (b) Cooper, P. D.; Kjaergaard, H. G.; Langford, V. S.; McKinley, A. J.; Quickenden, T. I.; Schofield, D. P. *J. Am. Chem. Soc.* **2003**, *125*, 6048.
- Andrews, L.; Ault, B. S.; Grzybowski, J. M.; Allen, R. O. *J. Chem. Phys.* **1975**, *62*, 2461.
- Chertihin, G. V.; Andrews, L. *J. Chem. Phys.* **1998**, *108*, 6404.
- (a) Thompson, W. E.; Jacox, M. E. *J. Chem. Phys.* **1989**, *91*, 3826. (b) Chertihin, G. V.; Saffel, W.; Yustein, J. T.; Andrews, L.; Neurock, M.; Ricca, A.; Bauschlicher, C. W. *J. Phys. Chem.* **1996**, *100*, 5261.
- Zhou, M. F.; Andrews, L. *J. Am. Chem. Soc.* **1998**, *120*, 11499.
- Frisch, M. J.; Trucks, G. W.; Schlegel, H. B.; Scuseria, G. E.; Robb, M. A.; Cheeseman, J. R.; Zakrzewski, V. G.; Montgomery, J. A., Jr.; Stratmann, R. E.; Burant, J. C.; Dapprich, S.; Millam, J. M.; Daniels, A. D.; Kudin, K. N.; Strain, M. C.; Farkas, O.; Tomasi, J.; Barone, V.; Cossi, M.; Cammi, R.; Mennucci, B.; Pomelli, C.; Adamo, C.; Clifford, S.; Ochterski, J.; Petersson, G. A.; Ayala, P. Y.; Cui, Q.; Morokuma, K.; Malick, D. K.; Rabuck, A. D.; Raghavachari, K.; Foresman, J. B.; Cioslowski, J.; Ortiz, J. V.; Baboul, A. G.; Stefanov, B. B.; Liu, G.; Liashenko, A.; Piskorz, P.; Komaromi, I.; Gomperts, R.; Martin, R. L.; Fox, D. J.; Keith, T.; Al-Laham, M. A.; Peng, C. Y.; Nanayakkara, A.; Gonzalez, C.; Challacombe, M.; Gill, P. M. W.; Johnson, B.; Chen, W.; Wong, M. W.; Andres, J. L.; Gonzalez, C.; Head-Gordon, M.; Replogle, E. S.; Pople, J. A. *Gaussian 98*, revision A.7; Gaussian, Inc.: Pittsburgh, PA, 1998.
- (a) Braidia, B.; Lauvergna, D.; Hiberty, P. C. *J. Chem. Phys.* **2001**, *115*, 90. (b) Gruning, M.; Gritsenko, O. V.; van Gisbergen, S. J. A.; Baerends, E. J. *J. Phys. Chem. A* **2001**, *105*, 9211. (c) Ghanty, T. K.; Ghosh, S. K. *J. Phys. Chem. A* **2002**, *106*, 11815. (d) Sodupe, M.; Bertran, J.; Rodriguez-Santiago, L.; Baerends, E. J. *J. Phys. Chem. A* **1999**, *103*, 166. (e) Xie, Y. M.; Schaefer, H. F.; Fu, X. Y.; Liu, R. Z. *J. Chem. Phys.* **1999**, *111*, 2532. (f) Jaramillo, J.; Scuseria, G. E.; Ernzerhof, M. *J. Chem. Soc.* **2003**, *118*, 1068.
- Braidia, B.; Hiberty, P. C.; Savin, A. *J. Phys. Chem. A* **1998**, *102*, 7872.

JA037125Z